Manuscript Details

Manuscript number	CEMCON_2018_587_R1
Title	Photocatalytic Concrete for NOx Abatement: Supported TiO2 efficiencies and impacts
Article type	Research paper

Abstract

The potential of TiO2-based photocatalysts in mitigating the effects of environmental pollutants is evident in the scientific literature but the large-scale implementation of photocatalytic concretes still appears limited, despite the current global concerns over urban NOx pollution. Improvements in cost-effectiveness are required to enhance the case for a photocatalyst-modified infrastructure and this must address catalyst efficiency, catalyst loading and performance durability. This paper compares photocatalytic efficiencies of TiO2 supported on mortar surfaces with the more conventional TiO2 dispersed in mortar. The influences of environmental conditions, such as NO concentration and flow rate, UVA light intensity and relative humidity, on photocatalytic performance are also investigated using photonic efficiency as an indicator. The supported TiO2 shows greater degradation of NOx (De-NOx), at about 9 times higher than TiO2 powder dispersed in the mortar, ca. 150 times higher utilization efficiency, than that of TiO2 in traditional photocatalytic mortar (with 5% loading).

Corresponding Author	Donald Macphee
Corresponding Author's Institution	University of Aberdeen
Order of Authors	Lu Yang, Amer Hakki, Li Zheng, Roderick Jones, Fazhou Wang, Donald Macphee
Suggested reviewers	andrea folli, Chi-sun Poon, Jos Brouwers

Submission Files Included in this PDF

File Name [File Type]

Cover letter for Revision.doc [Cover Letter]

Detailed Responses to Reviewers Comments (12-10-18).docx [Response to Reviewers]

highlights.doc [Highlights]

Graphical abstract.docx [Graphical Abstract]

Manuscript20181012-revised.docx [Manuscript File]

Revised Figures.docx [Figure]

Supporting Information-revised-20181012 (002).docx [Figure]

To view all the submission files, including those not included in the PDF, click on the manuscript title on your EVISE Homepage, then click 'Download zip file'.

Research Data Related to this Submission

There are no linked research data sets for this submission. The following reason is given:
Data will be made available on request

Dear Editor,

Thank you for the opportunity to submit a revised manuscript entitled "**Photocatalytic Concrete for NOx Abatement: Supported TiO_2 Efficiencies and Impacts**" (Manuscript No.: CEMCON_2018_587). We appreciate the positive and constructive comments and suggestions from you and the reviewer and have carefully revised our manuscript accordingly. We have also prepared a detailed response to the specific comments as a separate document (filename: Detailed Responses to Reviewers Comments). We hope that all these changes fulfill the requirements to make the manuscript acceptable for publication in **Cement and Concrete Research.**

We look forward to your positive response.

Sincerely yours,

Corresponding Author: Donald E Macphee.

E-mail address: d.e.macphee@abdn.ac.uk

Postal address: Department of Chemistry, University of Aberdeen, Meston Building, Meston Walk, AB24 3UE, Aberdeen, Scotland, United Kingdom

Ref.: CEMCON_2018_587

Title: Photocatalytic Concrete for NOx Abatement: Supported TiO_2 efficiencies and impacts

Journal: Cement and Concrete Research

Dear Editor,

Thank you and the reviewer for the helpful and constructive comments. We have addressed these in the detailed comments below and have incorporated the changes into the revised manuscript.

Editors and Reviewers' comments:

Reviewer 1:

This manuscript focuses on the NOx abatement of photocatalytic concrete by comparing TiO_2 dispersed in the mortar and applied at the surface. The NOx assessment is well executed by the authors, who have studied all the important parameters which can influence the photocatalytic process, more characterization of the concrete itself is required in order to understand the influence of the TiO_2 on the mortar.

The paper focusses on the performance of TiO_2 supported on exposed surface aggregates so the influence of the concrete is less significant than would be expected if the photocatalyst were embedded in the concrete. However, the relative performance of these supported photocatalyst systems has been expressed relative to that of a reference photocatalytic mortar in which the photocatalyst has been mixed into the mortar. The performance of this reference photocatalytic mortar is similar to photocatalytic mortar performances reported in the literature [e.g. Folli, et al., The Journal of Physical Chemistry Letters.2014, 5(5): 830-832].

It is important to stress that the performances reported in the literature are mainly expressed as changes in NOx concentration whereas our paper expresses performance in terms of photonic efficiency, an approach which normalizes results in terms of sample size and other measurement parameters, such as photon flux, gas flow rate, etc (see equation (1)); note also that the measurement conforms to ISO 22197-1: 2007. Typically, this number is much smaller than the percentage change in NOx concentration, i.e. a percentage change in NOx concentration of 8.3 % corresponds to a photonic efficiency of 0.1 %. For convenience, we express the performance of photocatalysts in both formalisms in the revised manuscript.

Therefore, the reviewers advise a major revision.

The amount of TiO_2 is set at 5%. This value seems to be completely arbitrary and the manuscript fails to explain why this amount has been selected. Moreover, the dispersion of the TiO_2 is not very well described in the manuscript.

There have been many studies of photocatalytic mortars, with TiO_2 concentrations ranging from 1 to 10 wt% TiO_2, expressed as a fraction of the cement mass [Brouwers, et al., Building and Environment 44 (2009) 2463–2474; Macphee, et al., Cement and Concrete Research 85(2016)48-54; Pacheco-Torgal, et al., Construction and Building Materials 25 (2011) 582–590; Hanus, et al., Progress in Materials Science 58 (2013) 1056–1102; Poon, et al., Environ. Sci. Technol. 43(2009) 8948–8952; Kurtis, et al., Cement and Concrete Research 60 (2014) 30–36; Lucas, et al., Cement and Concrete Research 43 (2013) 112–120 and so on]. Photocatalytic efficiency increases with photocatalyst loading up to around 5 wt% with further additions having only a small effect, also confirmed by our recent work (https://cordis.europa.eu/project/rcn/102057_en.html; EU-funded Light2CAT project which utilised a 4 wt% loading). We have selected 5 wt% based on this experience and have modified manuscript accordingly.

Efficient dispersion of photocatalyst particles in cements is challenging [Macphee and Folli, et al., Cement and Concrete Research 42 (2012) 539–548; Folli, et al, J Amer Ceram Soc, 93, (10), 3360-69, (2010), and other reports] but by adopting the techniques and conditions

used by others in the preparation of our reference mortars, and with their similarity in photocatalytic performance to those reported in the literature, we are confident that the microstructural characteristics of our reference materials are comparable with other photocatalytic mortars. Consequently, we have sought to separate the photocatalysts from the cement environment but to retain the advantages of the concrete infrastructure as a catalyst support. Our comparisons of supported catalyst systems with our reference can therefore be taken to be representative.

The manuscript is not focusing enough on the quality of the concrete itself, and the hydration mechanism affected by the tape, which should be a crucial discussion in an article talking about photocatalytic concrete.

We appreciate the reviewer's comment but believe that there is a misunderstanding in the perceived role of the mortar/concrete and of the tape used in placing the photocatalyst-coated sand. The primary objective of the approach is to provide a support for the catalyst enabling a separation of photocatalyst from the cement environment. Evidently, some photocatalyst does come into contact with concrete/mortar but a significant fraction is exposed only to the NOx contaminated air. There may be some benefits or disadvantages where photocatalsyts supported on the sand are close to the air/mortar interface but these are not quantitatively discussed.

The adhesive tape is used for the tape casting of TiO_2 coated sand onto the mortar surface. The sand is only pressed into the surface up to a maximum of two-thirds of its diameter so the tape does not come into contact with the cement and cannot affect the hydration chemistry of the cement.

We have strengthened these statements in the revised manuscript.

- The FTIR analysis is interesting, but the authors are drawing conclusions without further analyses. First, nothing is mentioned about the method used. Then, the difference is so small that it might be a measurement error. For instance, the Si-OH groups have the same absorption and the result might just be an increase in hydroxyl groups on the quartz

by the coating method conditions. Therefore all the speculation about there being Ti-O-Si bonds are not justified and should be proven by other characterization methods.

We have added more details on the FT-IR measurement and data analysis methods to the manuscript, specifically with regard to quantifying the important Ti-O-Si chemical linkages. There has now been quite a number of studies on this topic, including our own [Hakki, et al., Jove-Journal of Visualized Experiments, 2016, 125; Lu, et al, Applied Catalysis B-Environmental, 222(2018)200-208]. To illustrate the effect of Ti-O-Si more effectively on the general shape of the Si-O absorption around 960 cm^{-1}, we have included in the manuscript an FT-IR spectrum with the results of a deconvolution analyses (details provided in revised manuscript). The significance of the Ti-O-Si bonding, critical to the durability of the supported TiO_2 structures, is now more obvious. It may be noted also that the coating conditions (pH value around 4) does not appear to affect the quartz surface state.

- Authors say P8 "*Further discussions on measurement of the aggregate exposed depth and area will be presented in a subsequent paper*" and P10 "*It is not yet clear why but the effects of alkalinity, available at the composite-mortar interface, have previously been highlighted in offsetting a selectivity reduction linked to catalyst-support bonding via Ti-O-Si linkages*". However, this manuscript is already lacking novelty which means that these "further discussions" should be included in this paper in order to justify its publication.

Thank you for these comments. We have removed the reference to planned future papers made on p8 but we disagree with the reviewer with respect to the paper lacking novelty. The paper highlights several important findings:

- Previous inverse correlations observed for supported TiO_2 on quartz between nitrate selectivity and the degree of Ti-O-Si binding appear to be reversed in the present study. This is attributed to the higher local humidity to be expected in the close proximity of the cementitious material in the mortar and the consequent higher availability of

surface water on the catalyst, previously shown to enhance conversion of NO_2 to nitrate [Lu, et al, ACS Applied Materials & Interfaces, 9(2017)17035-17042].

- In supported structures, photocatalysts have shown NO and NOx abatement levels of around 9 times that of conventional mortars with less than a tenth of the TiO_2 loading.
- The sensitivity to real environmental variables, such as initial NO concentration, flow rate, light intensity and relative humidity, etc., are addressed to assist in decisions on for example, the placement of photocatalytic concrete elements.

We have strengthened the text to emphasise these novel outcomes.

- In overall, the NOx abatement results are not very convincing, since the absolute values of the NOx abatement and selectivity are rather low regardless of the coating. Moreover, some results such as the humidity causing a low reactivity have been shown numerous times in the literature [1][2][3] and cannot be used as "breakthrough results" in this paper. The discussion should focus more on the mechanism itself and how this new coating method influence and enhance the photocatalytic process.

We have already provided detailed mechanistic interpretations for NOx oxidation on these catalysts [Lu , et al, ACS Applied Materials & Interfaces, 9(2017)17035-17042] and have sought to show how those mechanisms can be supported utilizing the structures described in the present paper, i.e. the role of water in promoting nitrate selectivity and photocatalytic activity. The relative performance of the supported structures to that of embedded photocatalysts is convincingly demonstrated (Figure 7; see text above) with around 9 times improvement in NO and NOx abatement utilizing less than a tenth of the TiO_2 loading compared with conventional photocatalytic mortars. Based on our response to the reviewer's first point, regarding the reliability of our reference mortar, we believe that this significant performance improvement is representative and offers an approach to considerably improvements in the effectiveness of photocatalysts in construction applications.

References:

[1] M.M. Ballari, Q.L. Yu, H.J.H. Brouwers, Experimental study of the NO and NO_2 degradation by photocatalytically active concrete, Catal. Today. 161 (2011) 175–180. doi:10.1016/j.cattod.2010.09.028.

[2] H. Destaillats, M. Sleiman, D.P. Sullivan, C. Jacquiod, J. Sablayrolles, L. Molins, Key parameters influencing the performance of photocatalytic oxidation (PCO) air purification under realistic indoor conditions, Appl. Catal. B Environ. 128 (2012) 159–170. doi:10.1016/j.apcatb.2012.03.014.

[3] Q.L. Yu, M.M. Ballari, H.J.H. Brouwers, Indoor air purification using heterogeneous photocatalytic oxidation. Part II: Kinetic study, Appl. Catal. B Environ. 99 (2010) 58–65. doi:10.1016/j.apcatb.2010.05.032.

These useful papers also have been cited in our manuscript to state the importance of photocatalytic concrete and the humidity influences.

- Supported TiO_2 shows greater utilization efficiency than that of TiO_2 in mortar
- Binding durability of supported TiO_2 in mortar surface depends on its exposed depth
- Environmental conditions influences on photocatalytic performance are presented
- NO concentration, flow rate and relative humidity are main factors to NOx removal

Graphical abstract

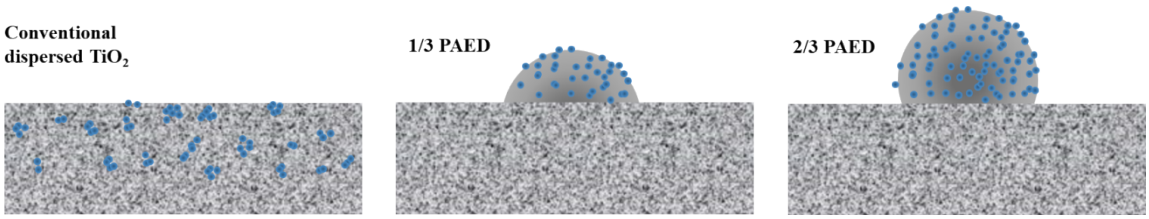

Photocatalytic Concrete for NOx Abatement: Supported TiO_2 Efficiencies and Impacts

Lu Yang[a,b], Amer Hakki[b], Li Zheng[c], M Roderick Jones[c], Fazhou Wang[*,a], Donald E Macphee[*,b]

[a] State Key Laboratory of Silicate Materials for Architectures, Wuhan University of Technology, 122# Luoshi Road, Wuhan 430070, China

[b] Department of Chemistry, University of Aberdeen, Meston Building, Meston Walk, AB24 3UE Aberdeen, Scotland, United Kingdom

[c] Concrete Technology Unit, Division of Civil Engineering, University of Dundee, DD1 4HN Dundee, Scotland, United Kingdom

Corresponding Author: fzhwang@whut.edu.cn (Fazhou Wang); d.e.macphee@abdn.ac.uk (Donald E Macphee).

Abstract: The potential of TiO_2-based photocatalysts in mitigating the effects of environmental pollutants is evident in the scientific literature but the large-scale implementation of photocatalytic concretes still appears limited, despite the current global concerns over urban NOx pollution. Improvements in cost-effectiveness are required to enhance the case for a photocatalyst-modified infrastructure and this must address catalyst efficiency, catalyst loading and performance durability. This paper compares photocatalytic efficiencies of supported TiO_2 on mortar surfaces with the more conventional TiO_2 dispersed in mortar. The influences of environmental conditions, such as NO concentration and flow rate, UVA light intensity and relative humidity, on photocatalytic performance are also investigated using photonic efficiency as an indicator. The supported TiO_2 shows greater degradation of NOx (De-NOx), at about 9 times higher than TiO_2 powder dispersed in the mortar, ca. 150 times higher utilization efficiency, than that of TiO_2 in traditional photocatalytic mortar (with 5% loading).

Keywords: Photocatalytic concrete; Supported TiO_2; NOx; Utilizations; Environmental Factors

1. Introduction

Despite the successful trialling of TiO_2 photocatalysts in several concrete applications [1-6], the widespread use of photocatalytic concretes for managing urban local air quality is still somewhat limited. Under solar illumination, TiO_2 can reduce ambient concentrations of nitrogen oxides (NOx) and other pollutants from automotive traffic and other combustion emissions, which can be in high concentrations at street level [7-9] and often exceed national exposure level guidelines. However, the key question is how to maximum the efficiencies and cost-effectiveness of incorporated photocatalysts in real environmental conditions. There are many reports identifying the efficacy of TiO_2 photocatalysts conventionally mixed into cementitious materials (with TiO_2 loadings from 1 to 10 wt% as a fraction of the cement content) [2, 4, 10-14]. Efficient dispersion of TiO_2 photocatalysts in cements is challenging due to the highly alkaline and calcium-rich cement environment. Such conditions promote TiO_2 agglomeration, reducing catalyst surface area, and surface precipitation of calcium hydroxide/calcium carbonate which may occluded underlying TiO_2 clusters [11, 18, 23]. The poor dispersibility and/or occlusion of TiO_2 by cement hydrates are likely to account for the high loadings, resulting in high cost and reduced efficiency of TiO_2 photocatalysts when intermixed into concrete.

An alternative approach is to attach the TiO_2 photocatalysts to a surface-exposed support rather than incorporating them in the concrete [24], which can give a controllable dispersibility and exposure of TiO_2 photocatalysts on concrete surfaces. Considering the stability, large-scale and low cost applications, our recent study [25] has focussed on the application of photocatalyst to granular quartz supports, and mounting these on to the surface of concrete (see Figure 1). The loading properties and photocatalytic activity of quartz-mounted TiO_2 photocatalysts showed that TiO_2 can be stably bonded on the substrate surface, and yield significant improvements in NOx degradation compared with TiO_2 powder. In addition to improved utilisation efficiency,

efficiency sensitivity to environmental factors, such as the UVA light intensity, relative humidity, and initial concentrations of pollutants, etc., must be addressed. Several laboratory-based studies have reported environmental effects [26, 27] but there are few reports specifically on the advantages of surface-supported TiO_2/concretes. The intensity of irradiation can also significantly affect photocatalytic activity and should be considered during calculating other environmental impacts. This paper quantitatively addresses these effects on supported TiO_2/concretes, utilising photonic efficiency [28, 29], a parameter which normalizes results in terms of sample size and other measurement parameters.

2. Experimental Procedure

2.1 Materials

Portland cement (CEM I, 52,5R) and ISO Standard sands (ISO 679: 2009, quartz sands) were used to prepare mortars. TiO_2/quartz sand aggregates were prepared using ISO Standard sands (1-2 mm) treated using a suspension of TiO_2 sol as described in ref [25]. The chemical compositions derived from X-ray fluorescence (XRF, Rigaku NEXQC$^+$) measurements of each product are given in Table 1. Commercial TiO_2 photocatalyst (PC105, CristalACTiV^{TM}) and acetone (C_3H_6OH, 99.9%, Sigma-Aldrich) were used as purchased. Mains water was used throughout the mortar preparation process.

(The position of Table 1)

2.2 Methods

2.2.1 Photocatalytic aggregate exposed mortar

Standard mortars were prepared according to BS EN197-1, using a Portland cement-sand-water mixture in the mass ratio of 1:3:0.5 (water/cement ratio = 0.5) as follows: Portland cement (450 ± 2) g and water (225 ± 1) g were blended in a mixing pot for 30 s at low speed (level 1) with Hobart mixer (N50, USA) after which sand (1350 ± 5) g was added. The resulting mixture was blended at the high speed (level 2) setting for another 30 s. Mortar slurries were then cast into

the moulds (50 mm width × 100 mm length × 20 mm height) and cured at room temperature under 100% relative humidity (RH) for 1 h.

Surface mounted, TiO_2-coated aggregate (QST, which has been prepared according to Ref [19], 1-2 mm) was applied to the freshly cast mortar, using the following method to ensure a monolayer could be achieved. TiO_2/quartz sand (QST) aggregates (ca. 10 g) were applied to adhesive tape (50 mm width × 100 mm length).The photocatalytic aggregate-coated tape was applied to the mortar surface such that the aggregates were forced into the mortar with constant pressures across the entire mortar area for 5s. The aggregate application was repeated such that two aggregate penetration depths were uniformly achieved: 1/3 aggregate exposure depth (1/3 AED, ca. 0.35 - 0.65 mm aggregate exposure height above mortar surface; applied pressure ~1514 g/50 cm^2), and 2/3 AED (ca. 0.65 – 1.3 mm AED above mortar surface; applied pressure ~343 g/50 cm^2) – see Figure 1. Following this, all samples were de-moulded after curing at room temperature and 100% RH conditions for 24 h, and further cured for 7 days.

Subsequently, the mortar top surface was immersed in acetone for 30 minutes and the adhesive tapes were removed from the aggregates. The obtained photocatalytic aggregate exposed mortar samples with 1/3 and 2/3 AED were denoted as 1/3PAED and 2/3PAED, respectively (Figure 1). The weight loss of aggregates were recorded for each aggregate support configuration (1/3PAED and 2/3PAED) enabling a comparison of binding performance. It should be noted that the tape, which is used for the tape casting of TiO_2 coated sand onto the mortar surface, does not come into contact with the cement and cannot affect the hydration chemistry of the cement.

For comparison, mortars were also prepared with TiO_2-free quartz sand aggregate (1-2 mm) exposed at 1/3 and 2/3 AED. These are denoted as 1/3AED and 2/3AED, respectively. Three mortar discs (50 mm width × 100 mm length × 20 mm height) were produced for each set.

(The position of Figure 1)

2.2.2 Photocatalyst blended mortar

Conventional TiO_2 photocatalyst blended mortar samples were also prepared to the same dimensions. The procedure used was similar to that described in Section 2.2.1 except that instead of tape casting the photocatalytic aggregate onto the pre-cast mortar, a ca. 2 mm thick layer of photocatalyst (TiO_2) blended mortar was applied. The photocatalyst (TiO_2) blended mortar was prepared as follows: TiO_2 powder (at 5% of the Portland cement mass) was mixed with Portland cement prior to blend with water for 30 s. The TiO_2 loading was selected based on literature reports which indicate that photocatalytic efficiency increases with photocatalyst loading up to around 5 wt% with further additions having only a small effect [15-22]. The sand was then added (cement: sand = 1 : 3, mass ratio), the mixture then being blended for another 30 s. The resulting photocatalyst blended mortar slurry was applied to the previously prepared mortar (50 mm width × 100 mm length × 20 mm height) such that a 2 mm thick photocatalytic surface layer was achieved. The products were cured at room temperature and 100% RH conditions for 7 days. The obtained photocatalyst blended mortar sample was denoted as 5%PM. Three mortar discs were produced for this sample.

2.2.3 Characterization

A calibration enabling TiO_2 loadings on quartz was obtained using XRF analysis of TiO_2:quartz sand ratios in mixtures in the range 0.1 to 50 wt. % TiO_2. In order to ensure the chemical bonding of TiO_2 to the support, i.e., quartz sand, Fourier transform infrared (FT-IR) spectra were recorded using a Perkin-Elmer Spectrum 2 spectrometer with 48 scans per sample collected from 400 to 4000 cm^{-1} at 1 cm^{-1} resolution. Prior to FT-IR testing, samples were ground and passed through a 75μm sieve and the Perkin-Elmer Spectrum 2 spectrometer was calibrated for background corrections. Obtained FT-IR spectra were subjected to peak deconvolution analyses as in our previous study [25]. The deconvolution parameters were fixed

for all samples and each deconvoluted peak was attributed according to literature assignations to specific bonded groups.

Morphologies of samples were observed by scanning electron microscope (SEM, Zeiss EVO MA10) equipped with an energy dispersive X-ray spectrometry (EDAX, Oxford INCA) for elemental composition analyses. The bonding strength of quartz sand on mortar surfaces with different exposure depth was tested by a pull-off test method, following ASTM D4541/D7234, using a PosiTest AT-A Automatic pull-off adhesion tester (Defelsko) with using 20 mm aluminum test dolly (maximum 24 MPa) and resin glue as an adhesive agent. According to the laboratory standard measurements, the 28 d compressive strength of this mortar is 52.7 MPa, and the pull out strengths of exposed quartz sands on mortar surface are ca. 4.0 MPa and ca. 1.2 MPa for 1/3 and 2/3 exposure depth, respectively.

2.3 Photocatalytic De-NOx performance

The photocatalytic performance of prepared samples (50 mm width × 100 mm length × 20 mm height) were measured in a flow-through reactor (ISO 22197-1: 2007), schematically illustrated in Figure 2. The test sample was placed inside the reactor so the NO gas had to flow over the sample surface. The sample was irradiated by a 500W Xe-lamp solar simulator (Sciencetech. Inc, Canada) light source. To investigate the influences of various environmental parameters on photocatalytic performance, including NOx concentrations, relative humidity and flow rates, etc., a series of concentrations (30, 70, 140, 250, 500, 1000 ppb) of NO gas in synthetic air, conditioned at a range of relative humidities (17% - 87% RH; measured using a HygroPalm 1 detector (Rotronic) at 25 ^{o}C), was passed at a volumetric flow rate of (0.83×10^{-5} – 13.3×10^{-5}) $m^3\ s^{-1}$ through the reactor. The concentrations of NO, NO_2 and NOx were measured by a Thermo Scientific Model 42i-HL High Level NO-NO_2-NOx Analyzer (Air Monitors Ltd., United Kingdom). Each sample was pre-conditioned under UVA light for over 5 hours to

removal the adsorbed organics. After this, the sample was placed in the flow through reactor and NOx measurements were taken in the dark until equilibrium concentrations were reached. After this, the evolution of NOx, NO and NO_2 concentrations under illumination were recorded until steady state concentrations were observed. The incident photon flux at the position of the sample was measured using a broadband thermopile detector (Gentec-EO-XLP12-3S-H2-D0). For comparison, the photocatalytic performances of pure quartz sand aggregate exposed mortar and photocatalyst blended mortar samples were measured under identical conditions. The photocatalytic efficiency (ξ) was calculated according to equation (1). The catalyst selectivity for nitrate (S%) was calculated according to equation (2).

$$\xi = \frac{(c_d - c_i)VP}{\Phi ART} \times 100\% \qquad (1)$$

$$S\% = \frac{\xi_{NO_X}}{\xi_{NO}} \times 100 \qquad (2)$$

Where c_d is the concentration in dark, c_i the concentration under illumination, V the volumetric flow rate, P the pressure, A the irradiated sample area, R the gas constant, T the absolute temperature and Φ the photon flux impinging the photocatalyst surface. The photocatalytic efficiency was determined separately for NO, NO_2 and total NOx.

It is important to stress that the performances reported in the literature are mainly expressed as changes in NOx concentration whereas our paper expresses performance in terms of photonic efficiency, an approach which normalizes results in terms of sample size and other measurement parameters, such as photon flux, gas flow rate, etc (see equation (1)). Typically, this number is much smaller than the percentage change in NOx concentration, i.e. a percentage change in NOx concentration of 8.3 % corresponds to a photonic efficiency of 0.1 % with the standard measure method and parameters in this study (ISO 22197-1: 2007). For convenience, the performance of photocatalysts in both formalisms are expressed in this study.

(The position of Figure 2)

2.4 Modelling

According to the descriptions of ISO 22197-1:2007, the photonic efficiency (ξ) is defined as the number of NO (NO_2) molecules transformed (produced) divided by the number of photons, impinging on the catalytic surface. Thus, the value of ξ depends on light irradiance, NO initial concentration, and flow rate at a certain relative humidity, as given in equation (1). The ISO 22197-1:2007 model gives the sample dimension (50 mm width × 100 mm length), the surface height to window (5 mm), the volumetric flow rate (5.0×10^{-5} m^3/s^{-1}), the light intensity (10 W/m^2) and as well as NO initial concentration (1 ppm) for laminar flow reactor. However, the flow rate (equivalent to a site wind speed) and flow characteristics (turbulent or laminar) are variable in real atmospheric conditions. To clarify the practicality of this laminar flow model, the upper limit flow rate was given by the following equation:

$$\mathrm{Re} = \frac{\rho_{air} u d_{reactor}}{\mu_{air}} = \frac{u d_{reactor}}{v_{air}} \qquad (3)$$

Where Re is the Reynolds number, laminar flow occurs when Re < 2300 for a pipe model; ρ_{air} is the density of the air (kg/m^3); u is the velocity of the air with respect to the object (m/s); $d_{reactor}$ is the hydraulic diameter (m), here for the slit equal to double height of reactor surface (10 mm); μ_{air} is the dynamic viscosity of the flow (kg/m.s); v is the kinematic viscosity of flowing air, here equal to 1.51×10^{-5} m^2/s.

Substituting the maximum Re value to eq. (3) yields 3.47 m/s (equal to a volume flow of 86 $\times 10^{-5}$ m^3/s) for the upper limit for laminar flow, which significantly exceeds experiment flow rates. Nevertheless, although the ISO method makes the basic assumption of no significant dependence on the mass transport of NO from the bulk to sample surface, several important reports imply that mass transport influences in ISO reactor should be taken into account, especially with high photocatalytic active surfaces and low NO flow rates [15, 26, 30-32]. The

contribution of the mass transport component can be predicted by the Peclet number (*Pe*), calculated using the following equations [33]:

$$Pe = \frac{L_{reactor} u}{D} = \mathrm{Re}_L \, Sc \qquad (4)$$

where $L_{reactor}$ is the characteristic length of active surface (0.01 m); *D* is the diffusion coefficient for NO (ca. 1.71×10^{-5} m^2/s); *Sc* is the Schmidt number, calculated from the ratio of *v*/D, 0.883.

3 Results and Discussion

3.1 Physio-chemical properties of photocatalysts

Figure 3 presents the surface morphologies and elemental analyses of pure and the TiO_2 modified quartz sands aggregates. The figure shows that TiO_2 particles (anatase crystalline phase, see Figure S1 in supplementary information) are still associated with the quartz sand support even after rigorous washing treatments (see the method of ref [25]) and agitation using ultrasound, demonstrating the robustness of the TiO_2 adhesion to the quartz surface and are reasonably well dispersed. The FT-IR spectra of pure quartz sand and TiO_2 modified quartz sand show a broad absorbance attributed to Ti-O-Si chemical linkages [28] (850 - 1000 cm^{-1}) suggesting a chemical bond between the support and TiO_2 particles (Figure 4); this peak is better differentiated by the peak deconvolution superimposed on the spectra (Figure 4 (b)); peaks at ca. 1070, 1090, 1117, and 1173 cm^{-1} are associated with the symmetric and asymmetric vibrations of Si-O-Si bonds, and the peak at ca. 940 cm^{-1} is attributed to Si-O-Ti bonds.

(The position of Figure 3)

(The position of Figure 4)

3.2 Aggregate binding performance

Table 2 presents the binding performance of pure and TiO_2 modified quartz sand aggregate on mortar surfaces with 1/3 AED or 2/3 AED configurations (Figure 1). It is noted that the lost percentage of quartz sand-TiO_2 composite (QST), defined as the weight difference upon removing the adhesive tape (Section 2.2.1), is greatest at the highest aggregate exposure depth,

i.e. 2/3 AED (2/3 PAED); with 2/3 of the diameter above the mortar; 1/3 AED gives the strongest adhesion to the mortar (1/3 PAED), which are also confirmed by the pull out strengths. This probably due to increased contact surface area but also, for rounded particles, because the greatest diameter lies beneath the mortar surface. Interestingly, the TiO_2 modified quartz sands have lower lost percentage than that of pure quartz sand on mortar surface with the same exposure levels (1/3AED and 2/3 AED). Presumably, TiO_2 particles supported on quartz further enhances the surface roughness and consequently the contact area to improve the physical retention of the aggregate support on the mortar surface.

(The position of Table 2)

3.3 Performance of supported TiO_2 on mortars

Figure 5 shows a typical concentration profile of NO, NO_2, and NOx for a QST sample exhibiting photocatalysis. Three stages can be observed: 1) NO and NOx concentrations stabilization without light illumination, 2) NO and NOx concentrations decrease with NO_2 concentration increasing upon illumination; a period of ~20 minutes is required to reach a steady state, 3) NO and NOx concentrations recover and NO_2 returns to zero after turning off the light. The photonic efficiency (ξ) for photocatalyst-induced concentration changes in NO, NOx and NO_2 can be calculated by using the above data in combination with eq. (1). On the assumption that NO_2 is further oxidised to NO_3^-, nitrate selectivity (S %) is obtained using eq (2). The De-NOx performance of prepared TiO_2 (TiO_2-H), commercial TiO_2 (TiO_2-C) and QST are shown in Figure 6.

(The position of Figure 5)

It can be noted that the prepared TiO_2 (TiO_2-H) has a higher ξ(NO) and nitrate selectivity than that of commercial TiO_2 (TiO_2-C). The higher nitrate selectivity drives a correspondingly higher NO_2 consumption rate. After being loaded on the aggregate surface, the supported TiO_2 (QST) presents a slight increase in De-NOx (0.62% ξ(NO), equal to ca. 51.4% NO removal)

with only a small decrease in nitrate selectively (37%). Significantly though, this performance is achieved with almost a third of the TiO_2 that was used for the TiO_2 (TiO_2-H)) powder, confirming that supported TiO_2 has greater utilization efficiency. A small reduction of nitrate selectively can be explained by our earlier findings [28, 34], which demonstrated that nitrate selectivity of TiO_2 can be reduced by Ti-O-Si linkages.

(The position of Figure 6)

The De-NOx performance of the QST photocatalysts on mortars is shown in Figure 7. Photonic efficiencies were significantly reduced with embedding into the mortar surface. It can be observed that the negative effects of embedding on photocatalysts are mainly associated with activity, which probably can be attributed to the reduction of available photocatalytic surface areas, and possibly also the influences of cement hydrates [12, 27]. It must also be noted however that the performance of the 2/3PAED is poorer than that of the 1/3PAED sample. This appears counter intuitive but may be associated with a shadowing effect, causing light intensity losses which offset against the increase in exposed catalyst surface area.

It can also be noticed that both aggregate exposed PAED (1/3PAED and 2/3PAED) samples show higher NO and NOx photonic efficiencies than that of traditionally prepared sample (5%PM), which are about 11 and 5 times higher for NO abatement, respectively, and 9 and 4 times higher for NOx abatement, respectively. It can be emphasised that the mass fraction of TiO_2 photocatalyst in QST is only 0.34%, again showing much higher utilization efficiency (150 times higher) than that of TiO_2 photocatalyst in traditional photocatalytic mortars (5% mass fraction). These observations have significant efficiency and economic impacts on the use of TiO_2 in photocatalytic concretes.

Comparison of Figures 6 and 7 show that nitrate selectivity (S%) of aggregate-supported TiO_2 is significantly enhanced when surface mounted on the mortar. It is not yet clear why but the effects of alkalinity, available at the composite-mortar interface, have previously been

highlighted in offsetting a selectivity reduction linked to catalyst-support bonding *via* Ti-O-Si linkages [39].

According to our previous results, Ti-O-Si linkages have shown negative effects on nitrate selectivity, attributed to the polarising influence of Si on the Ti-O bond. However, we have also previously shown the positive role of surface adsorbed water in conditioning nitrate selectivity of TiO_2 [28].

The availability of water to the TiO_2 surface is defined by local humidity; high humidity can lead to water condensation which would block active catalyst sites. The adsorbed water required to participate in NOx oxidation mechanisms is available even at low humidity but maintaining this level of humidity is important and this behavioural change (nitrate selectivity) in the proximity of the mortar substrate suggests that hydrated cement pastes, and its hydrophilic constituents, may contribute an important localised humidity control. In fact, the reduction in alkalinity arising from carbonation may reduce this enhancement; calcium carbonate is also less hydrophilic than $Ca(OH)_2$ and C-S-H gel and therefore less likely to favour an enhancement in water adsorption.

(The position of Figure 7)

3.4 The influences of environmental factors

In contrast to the expected levels of control of experimental variables in laboratory experiments, performance assessment of functional photocatalysts in the real environment must consider variations in influencing parameters such as initial NO concentration, flow rate, light intensity temperature and relative humidity. Before translating the laboratory performance of photocatalytic mortar (photonic efficiency, ξ) into quantifiable impacts on air quality (NOx/NO/NO_2 concentrations), the influences of these parameters on ξ should be assessed. Figure 8 shows how gas flow rate affects De-NOx photonic efficiency (ξ) of the photocatalytic

mortar (1/3PAED). It can be noted that whilst ξ(NOx) shows little variation, both ξ(NO) and ξ(NO_2 generation) do, with flow rate induced changes effectively cancelling out the change in ξ(NOx). However, an important observation here relates to the ξ(NO_2 generation) trend, which increases with flow rate. As NO_2 is significantly more toxic than NO, it is preferable to favour lower flow rates. This is confirmed in the %S data which indicate the highest conversion (of generated NO_2) to nitrate is at low flow rates. This is probably attributed to the mass transport effects of NO and NO_2 gas, as described by eq. (4). The high mass transport effects help to enhance the reaction time of pollutants on the supported photocatalysts and can be achieved by decreasing the Peclet number (Pe), a laminar flow rate dependent parameter.

(The position of Figure 8)

The influences of NO initial concentration on photonic efficiency are shown in Figure 9. It can be seen that ξ(NO), ξ(NO_2 generation) and ξ(NOx) increase with the increase of NO initial concentrations, but with different increasing rates. In the low initial NO concentration (< 140 ppb) range, the photonic efficiencies slightly increase with the increase of NO concentrations. However, when the initial NO concentration is greater than 250 ppb, as in real situations in major urban centers around the world, e.g. London, Beijing etc., [19], the photonic efficiencies increase rapidly, at least to 1 ppm NO (Figure 9). The interesting point in Figure 9 is that the *S*% dropped from ca. 85 % to ca. 59% as the initial NO concentration increased from within 140 ppb to over 250 ppb. Although there is no clear answer to explain the *S*% drop, several probable reasons can be deduced. The low NO volume fraction (below 140 ppb) will result in low coverage of the photocatalyst surface, which can decrease the reaction rate of NO molecules. On the contrary, high coverage (NO concentration over 250 ppb) will increase the reaction rate, corresponding to the NOx photonic trends in Figure 9. However, amongst these reactions, the NO_2 to NO_3^- reaction is influenced by the presence of physisorbed water [28]. A possible explanation for the drop in *S*% is that without proportionally increasing levels of

physisorbed water, the NO_2: physisorbed water ratio increases and reduces the oxidation rate of NO_2 to nitrate, thus decreasing the *S*%.

(The position of Figure 9)

Figure 10 shows the NO and NOx photonic efficiencies profiles of TiO_2 as a function of illumination intensity for a fixed TiO_2 loading. The reduction of photonic efficiency demonstrates that the utilization efficiency of incident photons decreases as incident UVA light intensity increases. Figure 10 suggests that photonic efficiency of NO_2 generation is independent of UVA irradiance, but the data represent the net effects on NO_2 concentration of NO oxidation and NO_2 consumption. The initial decrease in ξ(NO) means a reduced amount of generated NO_2 but in compensation for the constant ($\xi(NO_2)$ trend, the oxidation of NO_2 must also be reduced, i.e. so is also affected by illumination intensity. The *S*% is correspondingly decreased and indicate that weak UVA light intensity is sufficient to drive efficient NOx degradation.

(The position of Figure 10)

Figure 11 shows the effect of relative humidity on NOx degradation and nitrate selectivity. As previously reported [26, 27, 40-44], the NO and NOx photonic efficiencies are reduced as relative humidity is increased, giving a reduction in nitrate selectivity. However, it is also noted that generated $\xi(NO_2)$ does not change significantly with relative humidity and the small drop may be driven by a reduction in NO oxidation as suggested above. However, the increase in humidity is likely to bring about water condensation at the higher end of this range, especially at pore throats in the catalyst microstructure, this being expected to limit mass transport into the interparticle regions and restricting accessible surface. This means that a high relative humidity would strongly limit the photocatalytic efficiency.

(The position of Figure 11)

4 Conclusions

In this study, photocatalytic aggregate exposed mortars were prepared by using quartz sand supported TiO_2 (QST) composite as a photocatalytic functional aggregate. The physio-chemical properties, photocatalytic performance of QST and prepared mortars were identified. The results indicate that Ti-O-Si chemical linkages were formed and TiO_2 particles present uniform layers on quartz sand surface. The binding performance results indicate that TiO_2 modification can enhance the binding force between aggregate and cement hydrates, in which the lower aggregate exposure depth (AED) (most embedded configuration) can provide the higher binding stability. The QST sample shows greater photocatalytic utilization efficiency for degradation of NOx (De-NOx), which is about three times higher than for mortar dispersed TiO_2 powder.

Both QST exposed mortars show higher NO and NOx photonic efficiencies than that of traditional dispersion approach (5% TiO_2 in surface mortar layer). Most importantly, the mass fraction of TiO_2 in QST is only 0.34% of quartz sand mass, and shows a significantly higher utilization efficiency (ca. 150 times higher) than that of TiO_2 in traditional photocatalytic mortars, further confirming the efficiency and low-cost advantages of supported TiO_2 in photocatalytic concrete technology.

Considering the variability of real environmental conditions, such as initial NO concentration, flow rate, light intensity and relative humidity, etc., the identified influences of these parameters on photocatalytic performance should be managed, by selection of appropriate locations for application, to consider:

(1) ***Air flow rate***; low flow rates are preferred - NO and NO_2 removal can reach 80% under 0.375 L/min.

(2) ***NO concentration***; photonic efficiencies increase rapidly as initial concentration exceed 250 ppb, however *S*% drops to ca. 59% (from 85% at 140 ppb).

(3) ***UVA light intensity***; the highest photon utilization and nitrate selectivity was observed under weak UVA intensities (< 5 $mW.cm^{-2}$)

(4) ***Relative humidity***; high relative humidity strongly limits photocatalytic efficiency, probably due water condensation limiting mass transport (access to catalytic sites). However, at relative humidities lower than the dew point, surface water is known to enhance the rate of NO_2 oxidation [22].

5 Acknowledgements

The authors gratefully acknowledge funding from the UK Engineering and Physical Sciences Research Council (Grant Ref: EP/M003299/1) and the Natural Science Foundation of China (No. 51478370 and 51461135005) International Joint Research Project (EPSRC-NSFC).

6 References

[1] L. Cassar, A. Beeldens, N. Pimpinelli, G.L. Guerrini, Photocatalysis of cementitious materials, in: P.B.a.L. Casssar (Ed.) International RILEM Symposium on Photocatalysis, Environment and Construction Materials - TDP 2007, RILEM Publications SARL, Italy, 2007, pp. 131-145.

[2] M.J. Hanus, A.T. Harris, Nanotechnology innovations for the construction industry, Progress in Materials Science, 58 (2013) 1056-1102.

[3] L. Cassar, Photocatalysis of cementitious materials: Clean buildings and clean air, Mrs Bulletin, 29 (2004) 328-331.

[4] F. Pacheco-Torgal, S. Jalali, Nanotechnology: Advantages and drawbacks in the field of construction and building materials, Construction and Building Materials, 25 (2011) 582-590.

[5] E. Boonen, A. Beeldens, Recent photocatalytic applications for air purification in Belgium, Coatings, 4 (2014) 553-573.

[6] M.M. Ballari, H.J.H. Brouwers, Full scale demonstration of air-purifying pavement, Journal of hazardous materials, 254-255 (2013) 406-414.

[7] EU, Directive 2001/81/EC of the European Parliament and of the Council of 23 October 2001 on National Emission Ceilings for Certain Atmospheric Pollutants, (2001).

[8] Department for Environment Food & Rural Affairs, https://uk-air.defra.gov.uk/latest/currentlevels?period=24, 2017.

[9] Y. Zhu, J. Zhang, J. Wang, W. Chen, Y. Han, C. Ye, Y. Li, J. Liu, L. Zeng, Y. Wu, X. Wang, W. Wang, J. Chen, T. Zhu, Distribution and sources of air pollutants in the North China Plain based on on-road mobile measurements, Atmos. Chem. Phys., 16 (2016) 12551-12565.

[10] G. Hüsken, M. Hunger, H.J.H. Brouwers, Experimental study of photocatalytic concrete products for air purification, Building and Environment, 44 (2009) 2463-2474.

[11] D.E. Macphee, A. Folli, Photocatalytic concretes - The interface between photocatalysis and cement chemistry, Cement and Concrete Research, 85 (2016) 48-54.

[12] J. Chen, C.-S. Poon, Photocatalytic cementitious materials: Influence of the microstructure of cement paste on photocatalytic pollution degradation, Environmental Science and Technology, 43 (2009) 8948-8952.

[13] B.Y. Lee, A.R. Jayapalan, M.H. Bergin, K.E. Kurtis, Photocatalytic cement exposed to nitrogen oxides: Effect of oxidation and binding, Cement and Concrete Research, 60 (2014) 30-36.

[14] S.S. Lucas, V.M. Ferreira, J.L.B. de Aguiar, Incorporation of titanium dioxide nanoparticles in mortars - Influence of microstructure in the hardened state properties and photocatalytic activity, Cement and Concrete Research, 43 (2013) 112-120.

[15] M. Ballari, M. Hunger, G. Hüsken, H.J.H. Brouwers, NOx photocatalytic degradation employing concrete pavement containing titanium dioxide, Applied Catalysis. B: Environmental, 95 (2010) 245-254.

[16] E. Bocci, L. Riderelli, G. Fava, M. Bocci, Durability of NO Oxidation Effectiveness of Pavement Surfaces Treated with Photocatalytic Titanium Dioxide, Arabian Journal for Science and Engineering, 41 (2016) 4827-4833.

[17] A.M. Ramirez, K. Demeestere, N. De Belie, T. Mantyla, E. Levanen, Titanium dioxide coated cementitious materials for air purifying purposes: Preparation, characterization and toluene removal potential, Building and Environment, 45 (2010) 832-838.

[18] A. Folli, C. Pade, T.B. Hansen, T. De Marco, D.E. Macphee, TiO_2 photocatalysis in cementitious systems: Insights into self-cleaning and depollution chemistry, Cement and Concrete Research, 42 (2012) 539-548.

[19] E. Jimenez-Relinque, J.R. Rodriguez-Garcia, A. Castillo, M. Castellote, Characteristics and efficiency of photocatalytic cementitious materials: Type of binder, roughness and microstructure, Cement and Concrete Research, 71 (2015) 124-131.

[20] M. Smits, C.K. Chan, T. Tytgat, B. Craeye, N. Costarramone, S. Lacombe, S. Lenaerts, Photocatalytic degradation of soot deposition: Self-cleaning effect on titanium dioxide coated cementitious materials, Chemical Engineering Journal, 222 (2013) 411-418.

[21] C.S. Poon, E. Cheung, NO removal efficiency of photocatalytic paving blocks prepared with recycled materials, Construction and Building Materials, 21 (2007) 1746-1753.

[22] M.M. Ballari, M. Hunger, G. Husken, H.J.H. Brouwers, Heterogeneous Photocatalysis Applied to Concrete Pavement for Air Remediation, 2009.

[23] A. Folli, I. Pochard, A. Nonat, U.H. Jakobsen, A.M. Shepherd, D.E. Macphee, Engineering Photocatalytic Cements: Understanding TiO_2 Surface Chemistry to Control and Modulate Photocatalytic Performances, Journal of the American Ceramic Society, 93 (2010) 3360-3369.

[24] F.Z. Wang, L. Yang, H. Wang, H.G. Yu, Facile preparation of photocatalytic exposed aggregate concrete with highly efficient and stable catalytic performance, Chemical Engineering Journal, 264 (2015) 577-586.

[25] L. Yang, A. Hakki, F. Wang, D.E. Macphee, Photocatalyst efficiencies in concrete technology: The effect of photocatalyst placement, Applied Catalysis B: Environmental, 222 (2018) 200-208.

[26] M. Hunger, G. Hüsken, H.J.H. Brouwers, Photocatalytic degradation of air pollutants — From modeling to large scale application, Cement and Concrete Research, 40 (2010) 313-320.

[27] M.Z. Guo, T.C. Ling, C.S. Poon, Photocatalytic NOx degradation of concrete surface layers intermixed and spray-coated with nano-TiO_2: Influence of experimental factors, Cement & Concrete Composites, 83 (2017) 279-289.

[28] L. Yang, A. Hakki, F.Z. Wang, D.E. Macphee, Different Roles of Water in Photocatalytic DeNOx Mechanisms on TiO_2: Basis for Engineering Nitrate Selectivity?, ACS applied materials & interfaces, 9 (2017) 17035-17042.

[29] J.Z. Bloh, A. Folli, D.E. Macphee, Photocatalytic NOx abatement: why the selectivity matters, Rsc Advances, 4 (2014) 45726-45734.

[30] A. Mills, L. Burns, C. O'Rourke, S. Elouali, Kinetics of the photocatalysed oxidation of NO in the ISO 22197 reactor, J Photoch Photobio A, 321 (2016) 137-142.

[31] A. Mills, S. Elouali, The nitric oxide ISO photocatalytic reactor system: Measurement of NOx removal activity and capacity, J Photoch Photobio A, 305 (2015) 29-36.

[32] M.M. Ballari, M. Hunger, G. Hüsken, H.J.H. Brouwers, Modelling and experimental study of the NOx photocatalytic degradation employing concrete pavement with titanium dioxide, Catalysis Today, 151 (2010) 71-76.

[33] S.V. Patankar, Numerical Heat Transfer and Fluid Flow, New York, 1980.

[34] A. Hakki, L. Yang, F. Wang, D.E. Macphee, The Effect of Interfacial Chemical Bonding in TiO_2-SiO_2 Composites on Their Photocatalytic NOx Abatement Performance, Jove-Journal of Visualized Experiments, (2017).

[35] D.C.M. Dutoit, M. Schneider, R. Hutter, A. Baiker, Titania–Silica Mixed Oxides: IV. Influence of Ti Content and Aging on Structural and Catalytic Properties of Aerogels, Journal of Catalysis, 161 (1996) 651-658.

[36] J. Tokarský, P. Čapková, Structure compatibility of TiO_2 and SiO_2 surfaces, Applied Surface Science, 284 (2013) 155-164.

[37] M. Fujishima, H. Takatori, H. Tada, Interfacial chemical bonding effect on the photocatalytic activity of TiO_2–SiO_2 nanocoupling systems, Journal of Colloid and Interface Science, 361 (2011) 628-631.

[38] X. Gao, S.R. Bare, J.L.G. Fierro, M.A. Banares, I.E. Wachs, Preparation and in-Situ Spectroscopic Characterization of Molecularly Dispersed Titanium Oxide on Silica, J. Phys. Chem. B, 102 (1998) 5653-5666.

[39] M. Pérez-Nicolás, J. Balbuena, M. Cruz-Yusta, L. Sánchez, I. Navarro-Blasco, J.M. Fernández, J.I. Alvarez, Photocatalytic NOx abatement by calcium aluminate cements modified with TiO_2: Improved NO_2 conversion, Cement and Concrete Research, 70 (2015) 67-76.

[40] D. Seo, T.S. Yun, NOx removal rate of photocatalytic cementitious materials with TiO2 in wet condition, Building and Environment, 112 (2017) 233-240.

[41] J.K. Sikkema, S.K. Ong, J.E. Alleman, Photocatalytic concrete pavements: Laboratory investigation of NO oxidation rate under varied environmental conditions, Construction and Building Materials, 100 (2015) 305-314.

[42] M.M. Ballari, Q.L. Yu, H.J.H. Brouwers, Experimental study of the NO and NO_2 degradation by photocatalytically active concrete, Catalysis Today, 161 (2011) 175-180.

[43] Q.L. Yu, M.M. Ballari, H.J.H. Brouwers, Indoor air purification using heterogeneous photocatalytic oxidation. Part II: Kinetic study, Applied Catalysis B: Environmental, 99 (2010) 58-65.

[44] H. Destaillats, M. Sleiman, D.P. Sullivan, C. Jacquiod, J. Sablayrolles, L. Molins, Key parameters influencing the performance of photocatalytic oxidation (PCO) air purification under realistic indoor conditions, Applied Catalysis B: Environmental, 128 (2012) 159-170.

Figure Captions

Figure 1 Configurations for conventional TiO_2 dispersions in mortars and surface-mounted TiO_2-aggregate composites on photocatalytic mortar surfaces.

Figure 2 Configuration schematic of photocatalytic reaction for NOx degradation.

Figure 3 SEM morphologies and EDAX elements characteristics of (a) pure quartz sand, and (b) TiO_2 modified quartz sand aggregate.

Figure 4 (a) FT-IR spectrums of pure quartz sands and TiO_2 modified quartz sand aggregate; (b) TiO_2 modified quartz sand aggregate with component peaks identified by deconvolution in the wavenumber range 825 - 1350 cm^{-1}

Figure 5 Concentration profile of NO, NO_2 and NOx for QST sample during photocatalysis process.

Figure 6 De-NOx Photonic efficiencies and nitrate selectively of prepared TiO_2 (TiO_2-H), commercial TiO_2 (TiO_2-C), QST and QS samples.

Figure 7 De-NOx photonic efficiencies and nitrate selectively of 1/3PAED, 2/3PAED, 5%PM and (1/3 or 2/3) AED samples (photonic efficiency of aggregate exposed samples are normalised to 10 g aggregate weight).

Figure 8 De-NOx photonic efficiencies and S% of 1/3PAED with various NO flow rate.

Figure 9 De-NOx photonic efficiencies and S% of 1/3PAED with various initial NO concentrations.

Figure 10 De-NOx photonic efficiencies and S% of 1/3PAED with various irradiance.

Figure 11 De-NOx photonic efficiencies and S% of 1/3PAED with various relative humidity.

Tables

Table 1

Table 1 Chemical compositions of quartz sand and TiO_2 modified quartz sand aggregate

Chemical Composition (mass fraction, %)	Quartz Sand	TiO_2/Quartz Sand *
CaO	0.29	0.04
SiO_2	89.42	89.06
Al_2O_3	0.49	0.37
Fe_2O_3	0.07	0.09
MgO	0.04	0.02
MnO	-	-
TiO_2	0.02	0.36
K_2O	0.03	0.02
Na_2O	0.04	0.08
P_2O_5	0.01	0.01
Cl	0.01	-
SO_3	0.08	0.02

*To increase bonding forces, the quartz sands were treated by 0.1 M NaOH for 24 h before loading TiO_2

Table 2

Table 2 Binding performance of QS and QST aggregates on mortar with different AED

Item	Aggregate Weight and Lost Percentage (L.P.)			
	Initial/g	Remained/g	L.P./%	Average L.P./%
1/3PAED	9.23	7.81	15.4	17.0
	9.35	7.48	20.0	
	9.05	7.64	15.7	
2/3PAED	9.1	6.80	25.3	28.4
	9.65	6.90	28.5	
	9.4	6.44	31.5	
1/3AED	9.08	6.42	29.2	25.7
	9.22	7.26	21.2	
	9.24	6.76	26.8	
2/3AED	8.86	5.54	62.5	65.6
	8.74	6.99	79.0	
	8.69	4.81	55.3	

PAED: photocatalytic aggregate exposed mortar; AED: aggregate exposed mortar; 1/3 or 2/3: 1/3 or 2/3 aggregate exposed depth.

Figure 1

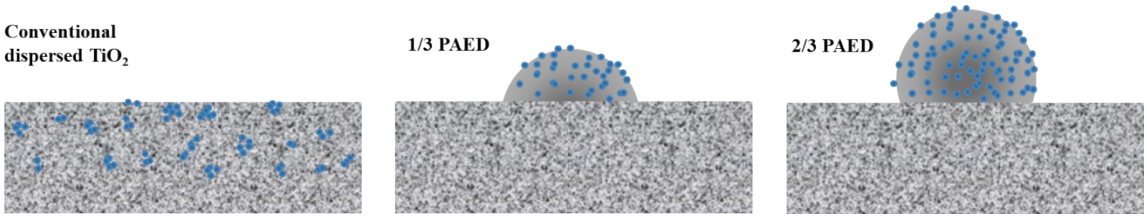

Figure 2

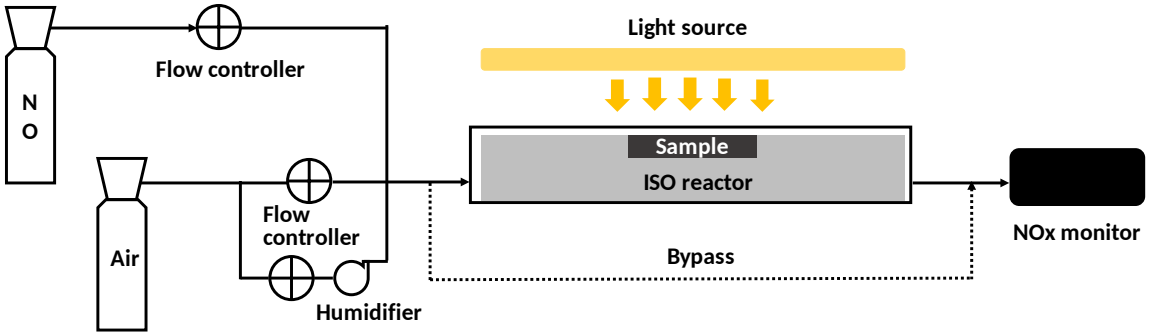
N
O
Flow controller
Light source
Sample
ISO reactor
NOx monitor
Air
Flow
controller
Humidifier
Bypass

Figure 3

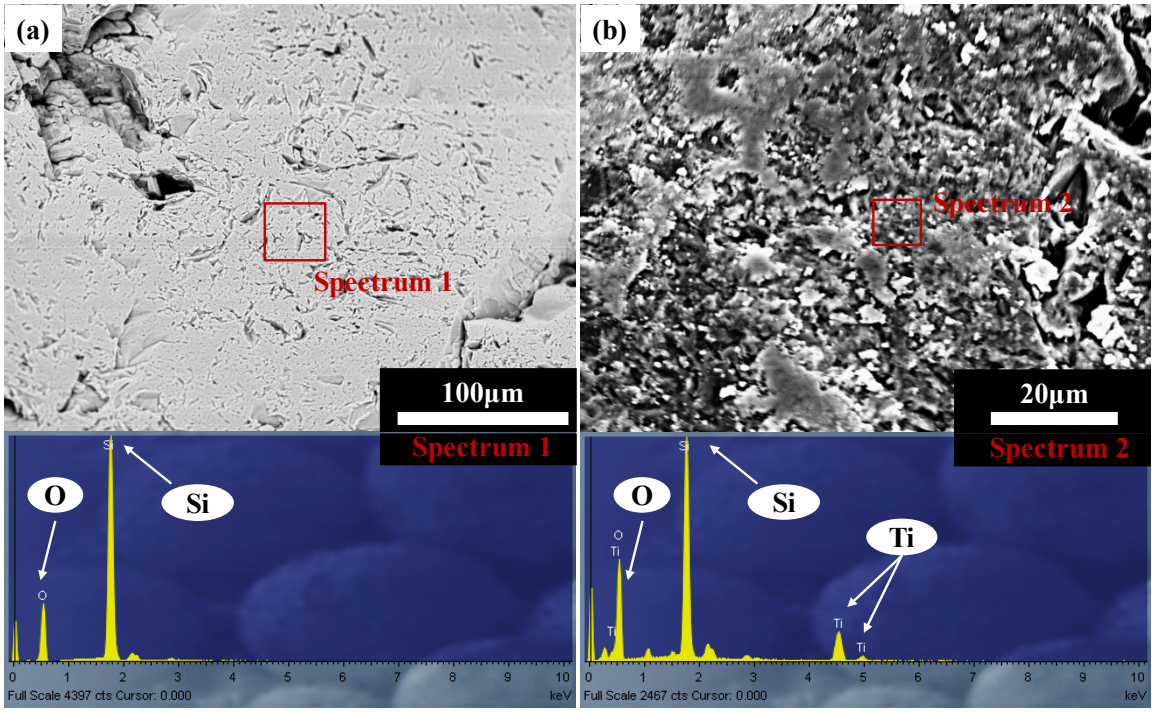
(a)
Spectrum 1
100µm
Spectrum 1
O
Si
Full Scale 4397 cts Cursor: 0.000
keV
(b)
Spectrum 2
20µm
Spectrum 2
O
Si
Ti
Full Scale 2467 cts Cursor: 0.000
keV

Figure 4

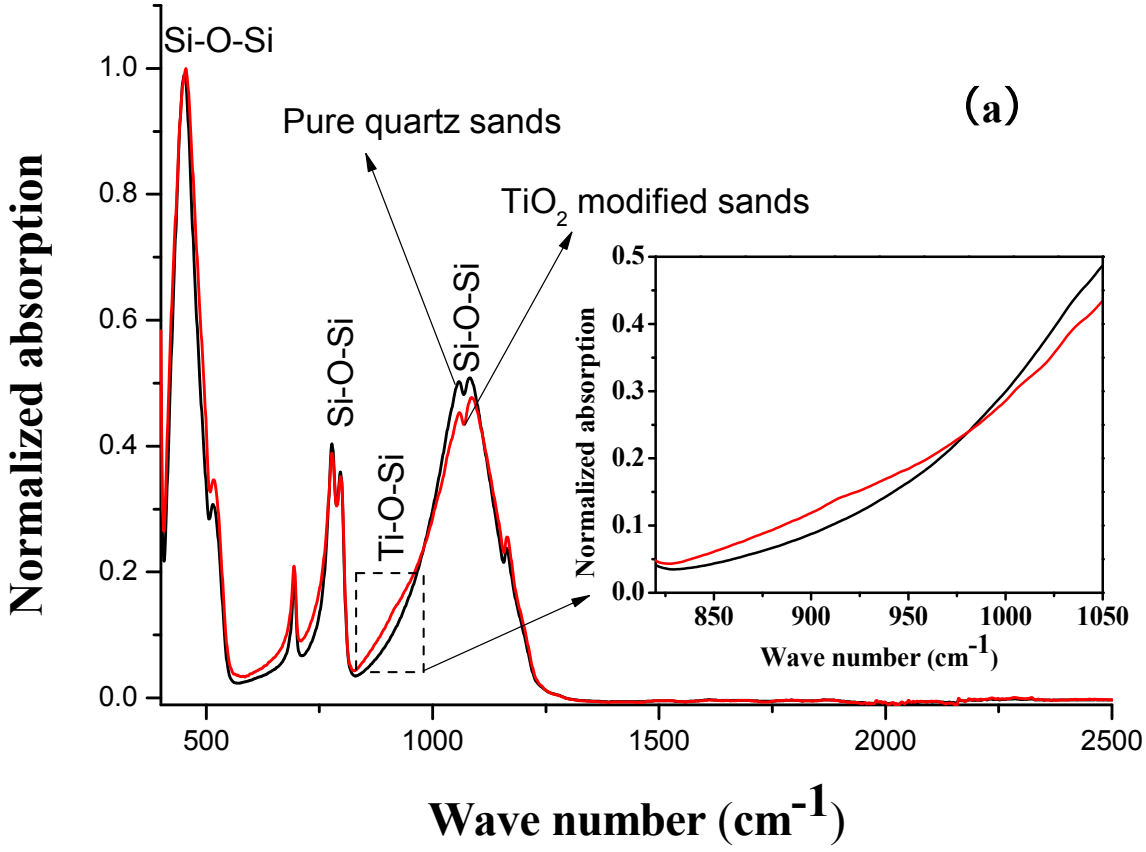
(a)
Si-O-Si
Pure quartz sands
TiO2 modified sands
Si-O-Si
Ti-O-Si
Si-O-Si
Normalized absorption
Wave number (cm-1)
Normalized absorption
Wave number (cm-1)

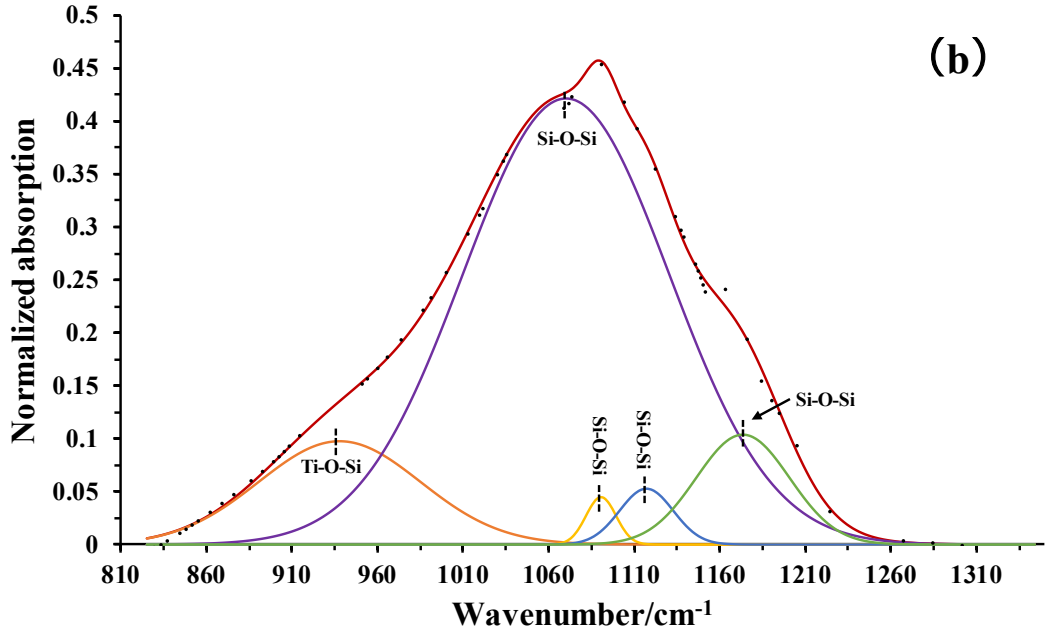
(b)
Si-O-Si
Ti-O-Si
Si-O-Si
Si-O-Si
Si-O-Si
Normalized absorption
Wavenumber/cm-1

Figure 5

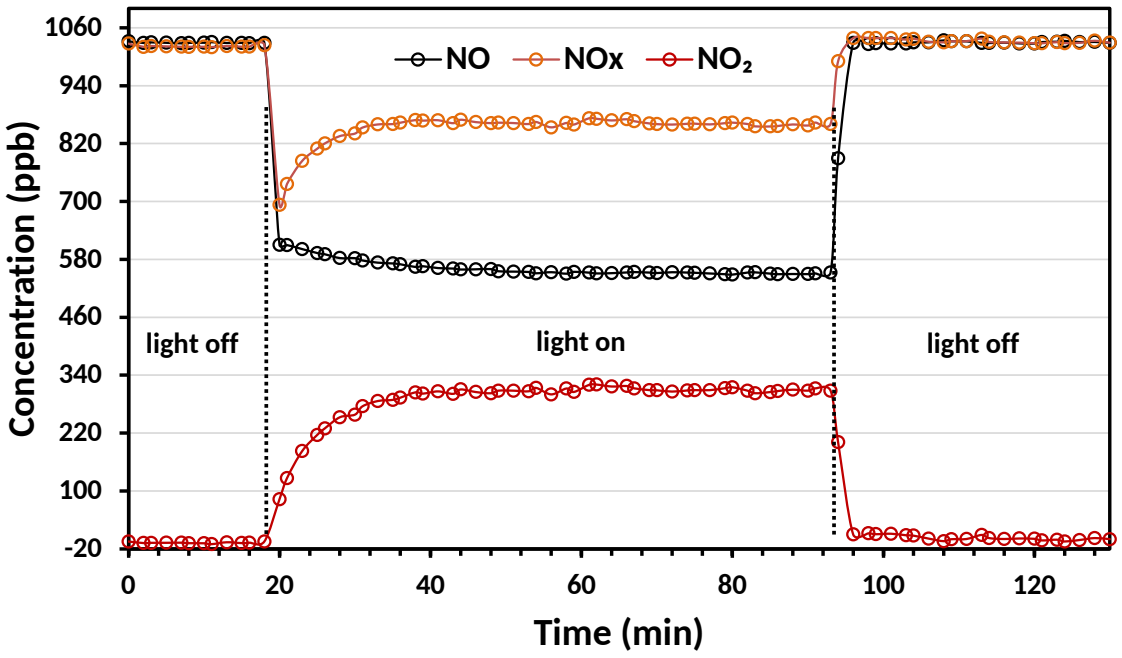
NO
NOx
NO2
Concentration (ppb)
1060
940
820
700
580
460
340
220
100
-20
light off
light on
light off
0
20
40
60
80
100
120
Time (min)

Figure 6

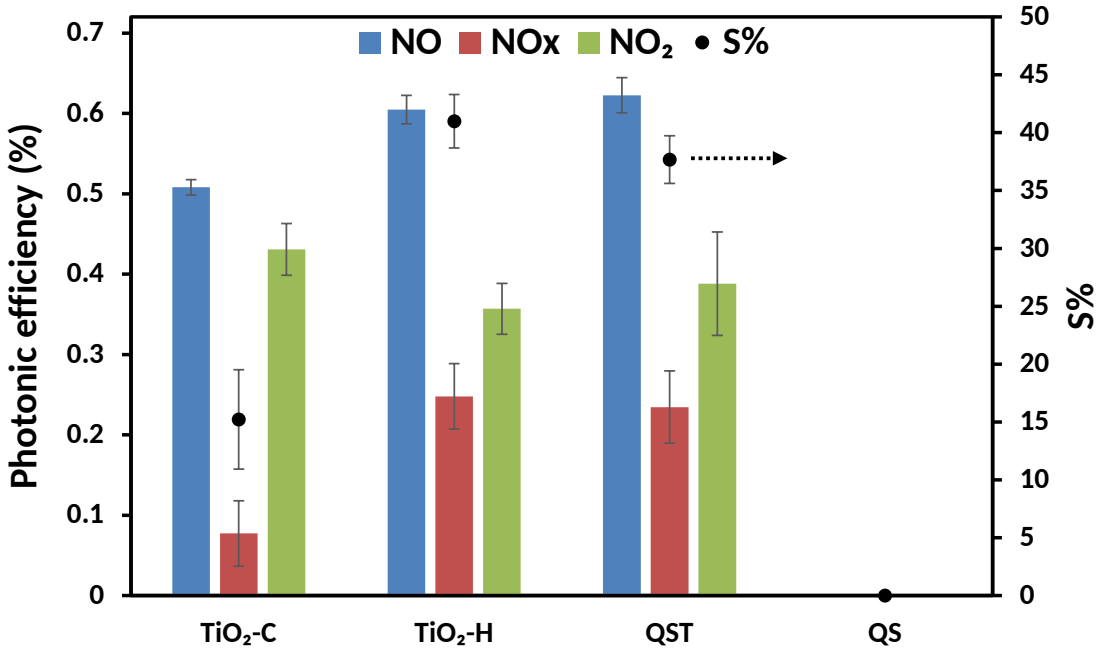
NO
NOx
NO2
S%
Photonic efficiency (%)
S%
0.7
0.6
0.5
0.4
0.3
0.2
0.1
0
50
45
40
35
30
25
20
15
10
5
0
TiO2-C
TiO2-H
QST
QS

Figure 7

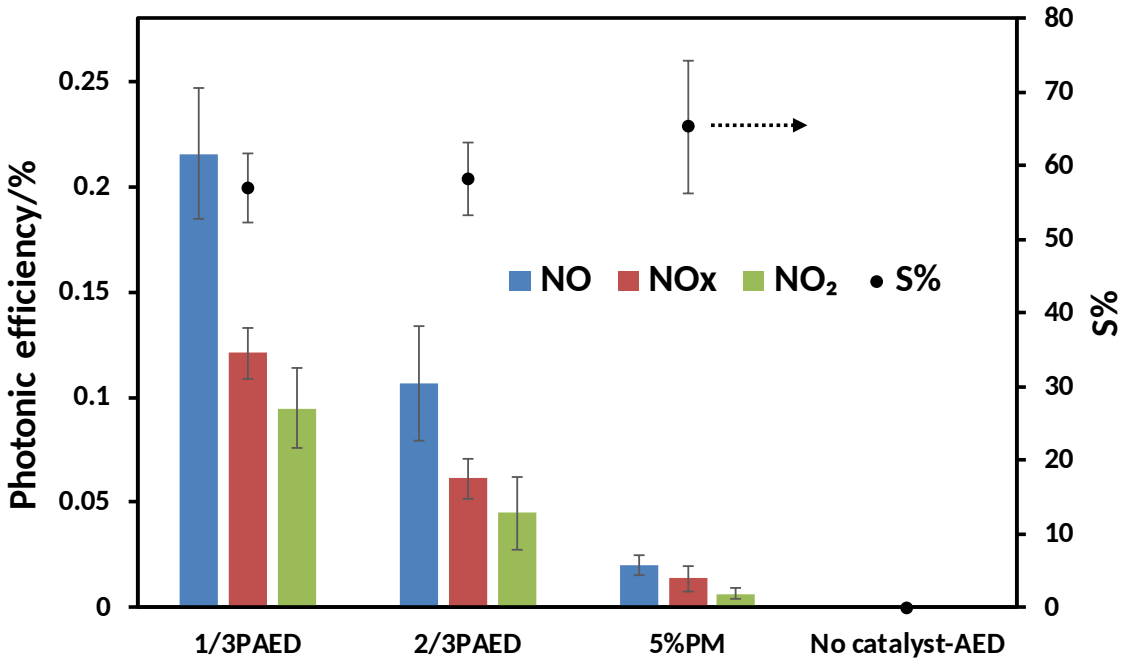
Photonic efficiency/%
0.25
0.2
0.15
0.1
0.05
0
80
70
60
50
40
30
20
10
0
S%
NO
NOx
NO₂
S%
1/3PAED
2/3PAED
5%PM
No catalyst-AED

Figure 8

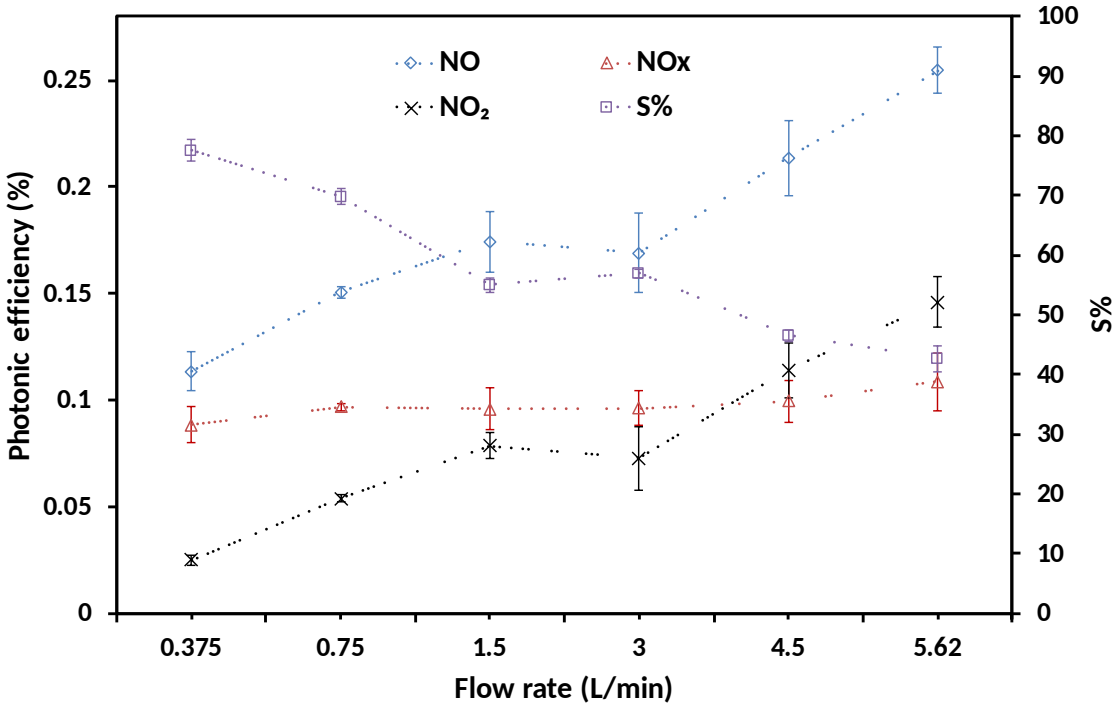
NO
NOx
NO₂
S%
Photonic efficiency (%)
S%
Flow rate (L/min)
0
0.05
0.1
0.15
0.2
0.25
0
10
20
30
40
50
60
70
80
90
100
0.375
0.75
1.5
3
4.5
5.62

Figure 9

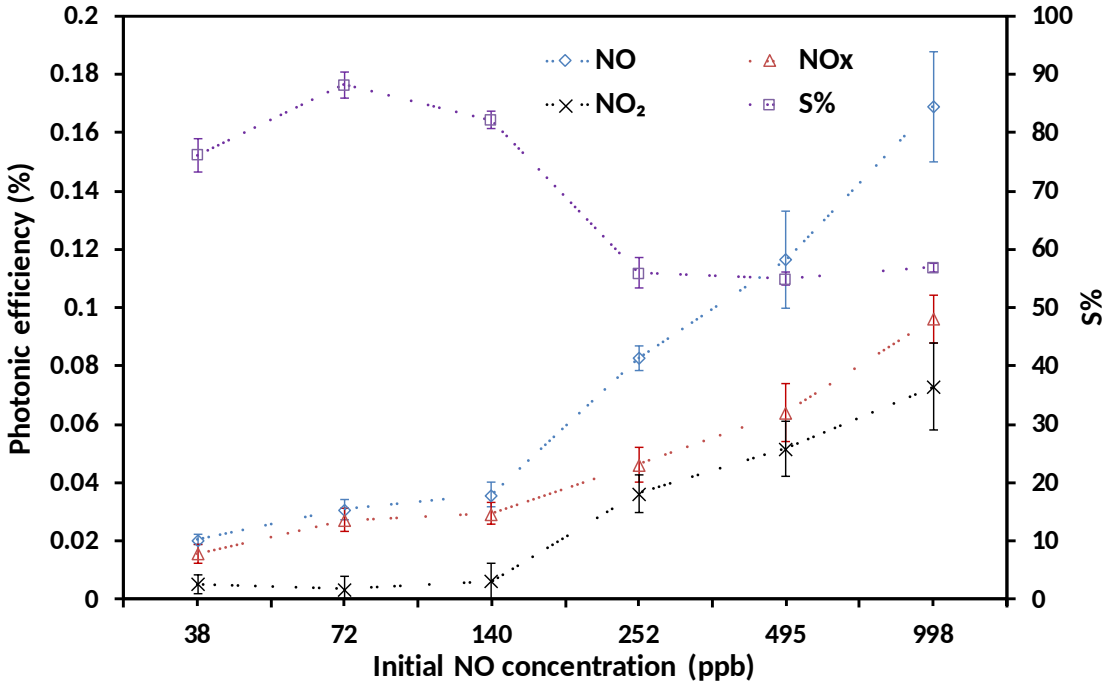
Photonic efficiency (%)
S%
Initial NO concentration (ppb)
NO
NOx
NO₂
S%
0.2
0.18
0.16
0.14
0.12
0.1
0.08
0.06
0.04
0.02
0
100
90
80
70
60
50
40
30
20
10
0
38
72
140
252
495
998

Figure 10

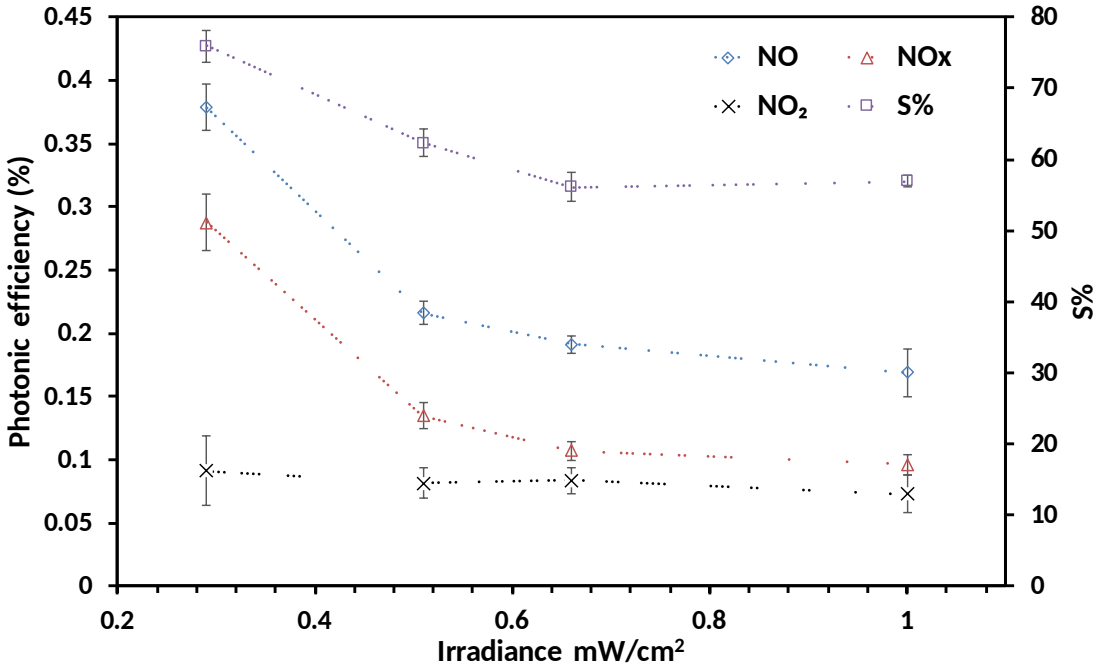
Photonic efficiency (%)
S%
Irradiance mW/cm2
NO
NOx
NO2
S%
0.45
0.4
0.35
0.3
0.25
0.2
0.15
0.1
0.05
0
80
70
60
50
40
30
20
10
0
0.2
0.4
0.6
0.8
1

Figure 11

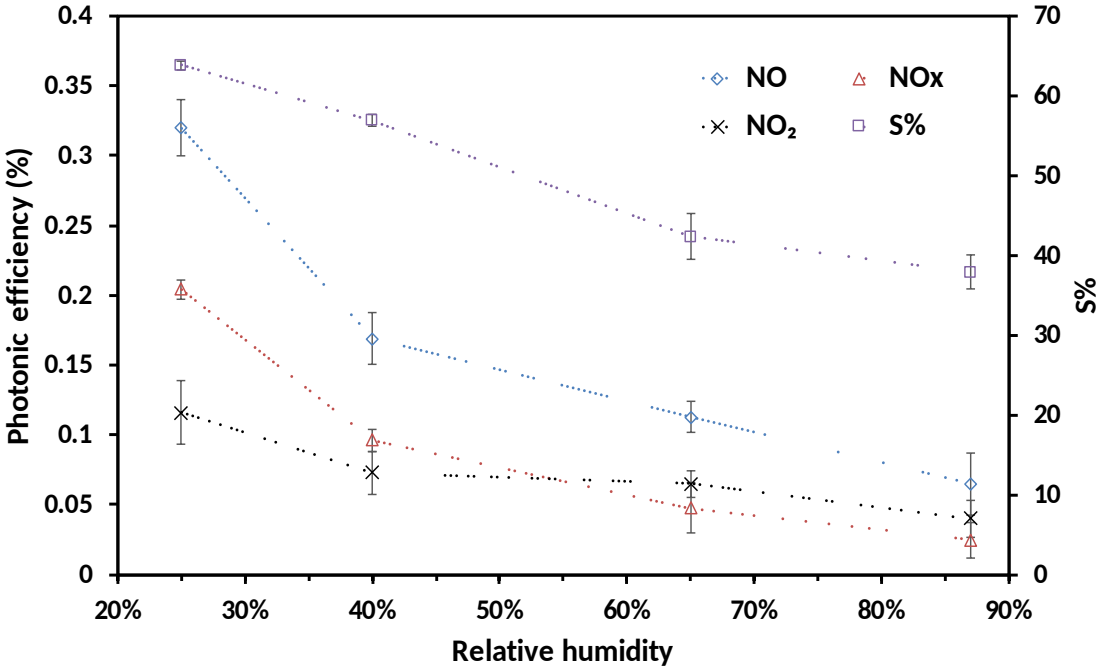
Photonic efficiency (%)
S%
Relative humidity
NO
NOx
NO2
S%
0.4
0.35
0.3
0.25
0.2
0.15
0.1
0.05
0
70
60
50
40
30
20
10
0
20%
30%
40%
50%
60%
70%
80%
90%

Supplementary Information for

Photocatalytic Concrete for NOx Abatement: Supported TiO_2 efficiencies and Impacts

Lu Yang[a,b], Amer Hakki[b], Li Zheng[c], M Roderick Jones[c], Fazhou Wang[*,a] , Donald E Macphee[*,b]

[a] State Key Laboratory of Silicate Materials for Architectures, Wuhan University of Technology, 122# Luoshi Road, Wuhan 430070, China

[b] Department of Chemistry, University of Aberdeen, Meston Building, Meston Walk, AB24 3UE Aberdeen, Scotland, United Kingdom

[c] Concrete Technology Unit, Division of Civil Engineering, University of Dundee, DD1 4HN Dundee, Scotland, United Kingdom

Corresponding Author: fzhwang@whut.edu.cn (Fazhou Wang); d.e.macphee@abdn.ac.uk (Donald E Macphee).

1. XRD analysis

The phase compositions of TiO_2 and photocatalytic quartz sand aggregate were determined by comparing X-ray diffraction (XRD) patterns, obtained on a PHILIPS P W 3O4O/60X' PertPRO diffractometer in the range 20 to 70 ° 2θ under Cu Kα radiation at a scanning speed of 6 ° min^{-1}, against reference XRD data.

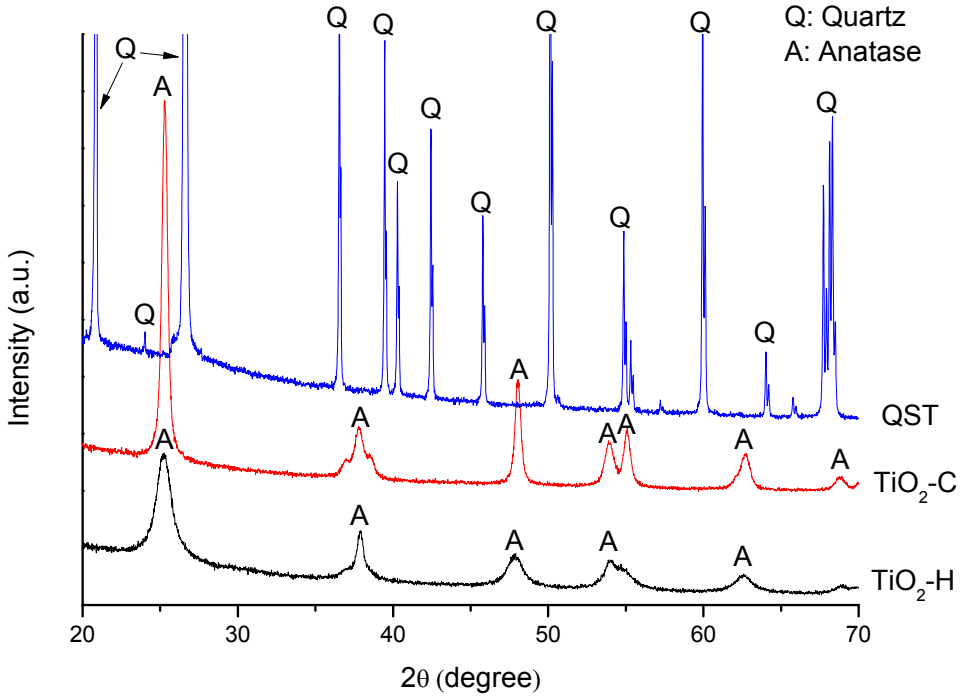

Figure S1 XRD patterns of the prepared TiO_2 particles (TiO_2-H), TiO_2/quartz sands (QST) aggregates and commercial TiO_2 (TiO_2-C)

Figure S1 shows the XRD patterns of the prepared TiO_2 particles, TiO_2/quartz sands (QST) aggregates and commercial TiO_2, respectively. It can be seen the prepared TiO_2 (TiO_2-H) and commercial TiO_2 (TiO_2-C) photocatalysts all present anatase crystalline phase with different relative intensities, while no obvious anatase peak can be observed in TiO_2 supported quartz sands aggregate. The loading amount of TiO_2 photocatalysts for QST sample therefore was

obtained by XRF, and the result shown the TiO_2 loading amount is 0.34% mass fraction to quartz sands aggregate (Table 1).

2. Photocatalytic De-NOx performance

The photocatalytic performance test method of prepared TiO_2 (TiO_2-H), commercial TiO_2 (TiO_2-C) were the same with that of photocatalytic quartz sand aggregate. The used amount of test sample was 0.1 g, which was uniformly distributed in a rectangular recess (area 5×10^{-3} m^2) inside the reactor. The TiO_2-H was obtained by drying the TiO_2 hydrosol (the preparation method can be seen in ref [1]) at 105 ^oC for 24 h. TiO_2-C is PC105 (CristalACTiV^{TM}).

[1] L. Yang, A. Hakki, F.Z. Wang, D.E. Macphee, Photocatalyst efficiencies in concrete technology: The effect of photocatalyst placement, Applied Catalysis B-Environmental, 222 (2018) 200-208.